sustainability

MDPI

Article

Spatiotemporal Dynamics of Carbon Sequestration Potential Across South Korea: A CASA Model-Based Assessment of NPP, Heterotrophic Respiration, and NEP

Nam-Shin Kim [1], Jae-Ho Lee [1] and Chang-Seok Lee [1,2,*]

[1] National Institute of Ecology, Seocheon 33657, Republic of Korea; geotop@nie.re.kr (N.-S.K.); jhlee14@nie.re.kr (J.-H.L.)
[2] Department Bio and Environmental Technology, Seoul Women's University, Seoul 01797, Republic of Korea
* Correspondence: restore0117@nie.re.kr or leecs@swu.ac.kr; Tel.: +82-41-950-5302

Abstract

Achieving carbon neutrality requires a comprehensive understanding of terrestrial carbon dynamics, particularly the capacity of ecosystems to act as carbon sinks. This study quantified the temporal and spatial variability of net primary production (NPP) and net ecosystem production (NEP) across South Korea from 2010 to 2024, assessing long-term carbon sink trends and their implications for carbon neutrality and nature-based solutions (NbSs). Using the Carnegie–Ames–Stanford Approach (CASA) model driven by Moderate Resolution Imaging Spectroradiometer (MODIS) satellite data and climate variables, we estimated ecosystem carbon fluxes at high spatial and temporal resolutions. In 2024, national NPP totaled 78.63 Mt CO_2 yr^{-1}, with a mean value of 1956.63 t CO_2 ha^{-1} yr^{-1}. High productivity was concentrated in upland forests of Gangwon-do, Mt. Jirisan, and northern Gyeongsangbuk-do, where favorable vegetation indices and climatic conditions enhanced photosynthesis. Lower productivity occurred in urbanized areas and intensively farmed lowlands. Heterotrophic respiration (RH) was estimated at 15.35 Mt CO_2 yr^{-1}, with elevated rates in warm, humid lowlands and reduced values in high-elevation forests. The resulting NEP in 2024 was 63.29 Mt CO_2 yr^{-1}, with strong sinks along the Baekdudaegan Range and localized negative NEP pockets in lowlands dominated by urban development or agriculture. From 2010 to 2024, the spatially averaged NPP increased from 1170 to 1543 g C m^{-2} yr^{-1}, indicating a general upward trend in ecosystem productivity. However, interannual variability was influenced by climatic fluctuations, land-cover changes, and data masking adjustments. These findings provide critical insights into the spatiotemporal dynamics of terrestrial carbon sinks in South Korea, offering essential baseline data for national greenhouse gas inventories and the strategic integration of NbSs into carbon-neutral policies.

Keywords: carbon neutrality; CASA model; net ecosystem production (NEP); net primary production (NPP); nature-based solutions (NbSs); terrestrial carbon sinks

check for updates

Academic Editor: Pablo Peri

Received: 14 September 2025
Revised: 8 October 2025
Accepted: 13 October 2025
Published: 24 October 2025

Citation: Kim, N.-S.; Lee, J.-H.; Lee, C.-S. Spatiotemporal Dynamics of Carbon Sequestration Potential Across South Korea: A CASA Model-Based Assessment of NPP, Heterotrophic Respiration, and NEP. *Sustainability* **2025**, *17*, 9490. https://doi.org/10.3390/ su17219490

Copyright: © 2025 by the authors. Licensee MDPI, Basel, Switzerland. This article is an open access article distributed under the terms and conditions of the Creative Commons Attribution (CC BY) license (https://creativecommons.org/licenses/by/4.0/).

1. Introduction

Global efforts to mitigate climate change have increasingly centered on achieving carbon neutrality, which has become a critical component in climate policy frameworks [1]. Carbon neutrality refers to a state in which net greenhose gas (GHG) emissions are zero, achieved by balancing anthropogenic emissions with equivalent removal or offsetting

measures [2]. This goal is fundamental for limiting the global temperature rise to 1.5–2 °C in line with the Paris Agreement.

Achieving carbon neutrality involves two complementary strategies: (1) minimizing emissions through measures such as transitioning to renewable energy, improving energy efficiency, adopting sustainable agricultural practices, and reducing waste; and (2) offsetting residual emissions through mechanisms that remove atmospheric CO_2, including reforestation, soil carbon sequestration, carbon capture and storage (CCS), and renewable energy projects [3,4]. Many governments, businesses, and organizations worldwide have pledged to reach carbon neutrality by 2050, underscoring its importance in the global climate agenda [5–7].

Historically, international climate policy and research have concentrated primarily on reducing emissions from industrial and energy sectors [6,8]. While technological innovation remains essential for mitigation, climate strategies must also incorporate measures for absorbing and removing existing emissions [9]. In this context, nature-based approaches serve as a vital safety net, providing multiple co-benefits beyond carbon sequestration, such as biodiversity conservation and ecosystem resilience [10–12].

Carbon sinks—systems that absorb more CO_2 than they emit—are indispensable for offsetting residual emissions from hard-to-abate sectors such as agriculture and heavy industry. These sinks can be natural, including forests, oceans, and soils, or artificial, involving technological interventions. They have long played a fundamental role in regulating the Earth's carbon cycle and are increasingly recognized as key mechanisms for achieving net-zero targets [13–15].

As global warming accelerates, understanding terrestrial carbon cycling has become a scientific priority. Terrestrial ecosystems act as major carbon sinks, sequestering atmospheric CO_2 and thereby supporting global carbon neutrality objectives [13,16,17]. Consequently, developing robust systems to quantify and monitor ecosystem carbon absorption over the long term is imperative. Among available metrics, net ecosystem production (NEP) is a key indicator of an ecosystem's carbon sequestration capacity. NEP is defined as the difference between net primary productivity (NPP)—carbon fixed by photosynthesis—and heterotrophic respiration (RH)—CO_2 released by soil microbial activity [18–21].

Traditional NEP estimation methods often relied on ground-based measurements of carbon fluxes, limiting their applicability for large-scale and long-term assessments. To address these limitations, remote sensing–based modeling approaches have gained prominence. The Carnegie–Ames–Stanford Approach (CASA) model is widely employed for estimating ecosystem carbon fluxes by integrating Moderate Resolution Imaging Spectroradiometer (MODIS) satellite-derived variables (e.g., NDVI) with climate drivers such as solar radiation, temperature, and evapotranspiration [22–26]. CASA estimates NPP by incorporating vegetation-specific maximum light-use efficiency (ε_{max}) and accounting for climate stress factors, enabling spatially explicit and temporally resolved analyses of carbon dynamics [27–29]. Owing to these advantages, CASA is widely applied in carbon monitoring programs across Asia, North America, and Europe, and is recognized in the IPCC [30] guidelines as a Tier 3 methodology for national greenhouse gas inventories [31–33].

South Korea presents a particularly complex context for carbon accounting due to its heterogeneous land-use mosaic of temperate forests, agricultural lands, and urban areas, where NEP exhibits high spatiotemporal variability driven by vegetation dynamics and climate variability [18,34]. However, most existing studies on NEP in Korea are limited to short-term or site-specific analyses [35], and high-resolution, long-term national assessments remain scarce. This gap constrains the accurate evaluation of carbon neutrality strategies and the integration of nature-based solutions (NbSs) into national climate policies.

This study has the following aims: (1) to quantify the temporal and spatial variability of NPP and NEP across vegetation types and climate drivers in South Korea; (2) to identify long-term carbon sink trends from 2010 to 2024; and (3) to explore regional implications of NEP distribution in the context of carbon neutrality and NbSs. The results are expected to provide essential baseline data for enhancing national greenhouse gas inventories, informing regional carbon management strategies, and supporting the scientific basis of future carbon-neutral policies.

2. Materials and Methods

2.1. Study Area

This study was conducted on terrestrial ecosystems across South Korea (Figure 1). The study covers all terrestrial ecosystems included in the national land-cover database, such as forests, croplands, grasslands, wetlands, and built-up areas.

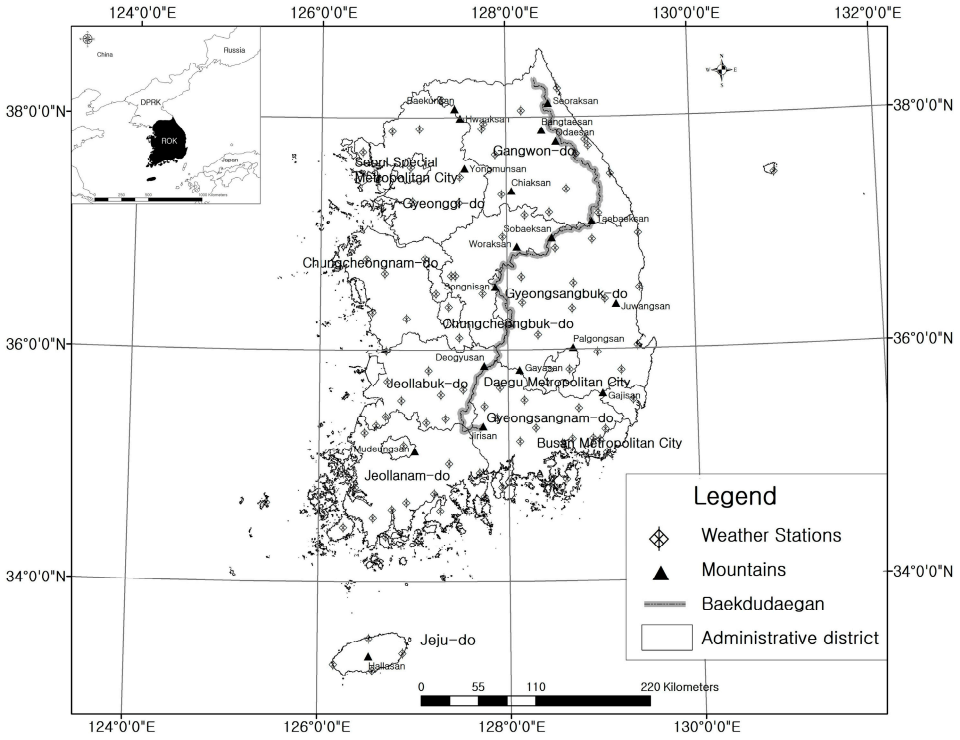


Figure 1. Spatial distribution of the 97 meteorological station sites used for generating climate surfaces in South Korea. These stations provided daily observations of temperature, precipitation, and solar radiation from 2010 to 2024.

2.2. Materials

2.2.1. Meteorological Data

Daily observations of air temperature, precipitation, and solar radiation from 97 Korea Meteorological Administration stations (2010–2024) were quality-controlled, aggregated to monthly/annual steps, and interpolated to continuous raster layers aligned with the 250 m grid (Figure 1). Established geostatistical approaches suitable for high-resolution climate surfaces from sparse networks were considered (e.g., kriging, thin-plate spline, Inverse Distance Weighting) [36,37].

2.2.2. Maximum Light Use Efficiency Data

A vegetation-type map was used to assign ε_{max} values across South Korea at 250m resolution. Representative biome-level ε_{max} values (g C MJ^{-1}) for grassland, conif-

erous, deciduous broadleaf, and mixed forest follow published LUE calibrations and the study's Table 1 [32,38–41].

Table 1. Maximum light use efficiency (ε_{max}) by vegetation type.

Vegetation Type	ε_{max} (gC·MJ^{-1})
Grassland	0.860
Coniferous Forest	0.962
Deciduous Broadleaf Forest	1.165
Mixed Forest	1.051

2.3. Methods

2.3.1. Estimation of Net Primary Production (NPP)

According to Equation (1), Monthly NPP at pixel p and month m was modeled within a CASA-type light-use-efficiency (LUE) framework [22,38–41]:

$$NPP_{p,m} = APAR_{p,m} \times \varepsilon_{max,p} \times T_{scalar,p,m} \times W_{sclar,p,m} \quad (1)$$

where ε_{max} is the biome-specific maximum LUE (g C MJ^{-1}). T_{scalar} and W_{scalar} (both $\in [0, 1]$) down-regulate productivity due to thermal and water limitations, respectively.

APAR was computed as in [38] and according to Equation (2),

$$APAR_{p,m} = 0.5 \times S_{r,p,m} \times FPAR_{p,m} \quad (2)$$

where Sr is the monthly shortwave radiation sum (MJ m^{-2} month^{-1}) and the factor 0.5 converts shortwave to photosynthetically active radiation (PAR). FPAR (Fraction of Photosynthetically Active Radiation) was derived from MODIS NDVI (MYD13Q1 v6.1; scale factor $\times 0.0001$) using a bounded linear transform to limit saturation [42]: According to Equation (3),

$$FPAR_{p,m} = \min(FPAR_{max}, \max\left(FPAR_{min}, \frac{NDVI_{p,m} - NDVI_{min}}{NDVI_{max} - NDVI_{min}}\right)) \quad (3)$$

Note: The NDVI values above are reached after applying the $\times 0.0001$ scale factor; thresholds are $NDVI_{min}$ = 0.10, $NDVI_{max}$ = 0.86, $FPAR_{min}$ = 0.001, and $FPAR_{max}$ = 0.95.

Temperature limitation followed the CASA practice of scaling monthly mean air temperature to [0, 1] relative to biome-appropriate thresholds [38,39]. Water limitation was expressed as an evaporative—fraction proxy using MODIS ET/PET (MOD16A2GF v6.1) harmonized to the analysis grid [43]. According to Equation (4),

$$W_{scalar,p,m} = \min(1, \max\left(0, \frac{ET_{p,m}}{PET_{p,m}}\right)) \quad (4)$$

where 8-day ET and PET (kg m^{-2} $\approx$ mm) were summed to monthly totals prior to establishing the ratio. This aligns canopy water stress with atmospheric demand and avoids NDWI-only approximations [44].

The LUE formulation and class-wise assignment of ε_{max} follow published practice and Table 1 [32,38–41]. Monthly NPP outputs are in g C m^{-2} month^{-1} and are summed to g C m^{-2} yr^{-1} for annual totals.

2.3.2. Empirical Modeling of Heterotrophic Respiration (RH)

Monthly RH was estimated with a climate-response function that captures exponential temperature sensitivity and a saturating precipitation effect: According to Equation (5),

$$RH_{p,m} = \mathrm{k} \times \left[exp\left(a \times T_{p.m}\right) + ln\left(b \times P_{p,m} + 1\right)\right] + d_m \times r_h \quad (5)$$

where T is monthly mean air temperature (°C); P is monthly precipitation (mm); d_m is the number of days per month; and k is the light extinction coefficient, which regulates the attenuation of photosynthetically active radiation within the canopy. a and b are empirical coefficients used in the CASA-type model to parameterize the temperature and moisture stress functions, respectively. r_h heterotrophic respiration = (0.22, 0.0913, 0.3145, 0.465). The formulation is consistent with large-scale soil respiration syntheses and applications [44,45].

2.3.3. Calculation of Net Ecosystem Production (NEP)

Annual NEP was computed as follows, according to Equation (6):

$$NEP_{p,y} = \sum_{m=1}^{12} NPP_{p,m} - \sum_{m=1}^{12} RH_{p,m} \quad (6)$$

where positive values indicate net carbon uptake. Carbon quantities were converted to CO_2 using the IPCC molecular–weight ratio (1 g C = 3.67 g CO_2); maps are reported in t CO_2 $ha^{-1}yr^{-1}$ [30].

2.3.4. Spatial Aggregation Procedure

Pixel-level NEP was aggregated to municipality-level units (si/gun/gu) using area-weighted means across vegetation classes; non-vegetated pixels were excluded uniformly across years. For agricultural land, sector-specific absorption coefficients were adopted to ensure compatibility with national and IPCC sectoral accounting [30].

2.3.5. Input Datasets and Analytical Resolution

All inputs were harmonized to a common 250 m grid (EPSG:5186) for pixel-wise integration. MODIS MYD13Q1 NDVI (250 m, 16-day) and MOD16A2GF ET/PET (500 m, 8-day) were reprojected and resampled to 250 m, with product scale factors applied (NDVI × 0.0001; ET/PET × 0.1) and monthly compositing via a Julian-day grouping scheme [42,43].

The satellite imagery and meteorological data were analyzed using ArcGIS 10.8 (Esri, Redlands, CA, USA).

3. Results

3.1. Net Primary Production (NPP)

In 2024, total NPP in South Korea was estimated at 78.63 Mt CO_2 yr^{-1}, with a national mean of 56.63 t CO_2 ha^{-1} yr^{-1} (equivalent to 1543 g C m^{-2} yr^{-1}). Spatial patterns reveal pronounced concentrations of high productivity in the upland forests of Gangwon-do, the Mt. Jirisan region, and the northern mountains of Gyeongsangbuk-do (Figure 2). These areas, dominated by coniferous and deciduous broadleaved forests, exhibit elevated vegetation indices (e.g., NDVI), higher ε_{max} values, and favorable temperature (Tscalar) and moisture (Wscalar) conditions, collectively enhancing photosynthetic capacity. By contrast, lower NPP occurs across the western coastal plains of Jeollanam-do, agricultural zones in the Nakdong River basin, and the Seoul Metropolitan Area, where impervious surfaces and sparse vegetation suppress productivity. In urban cores, some grid cells approach zero due to minimal green cover.

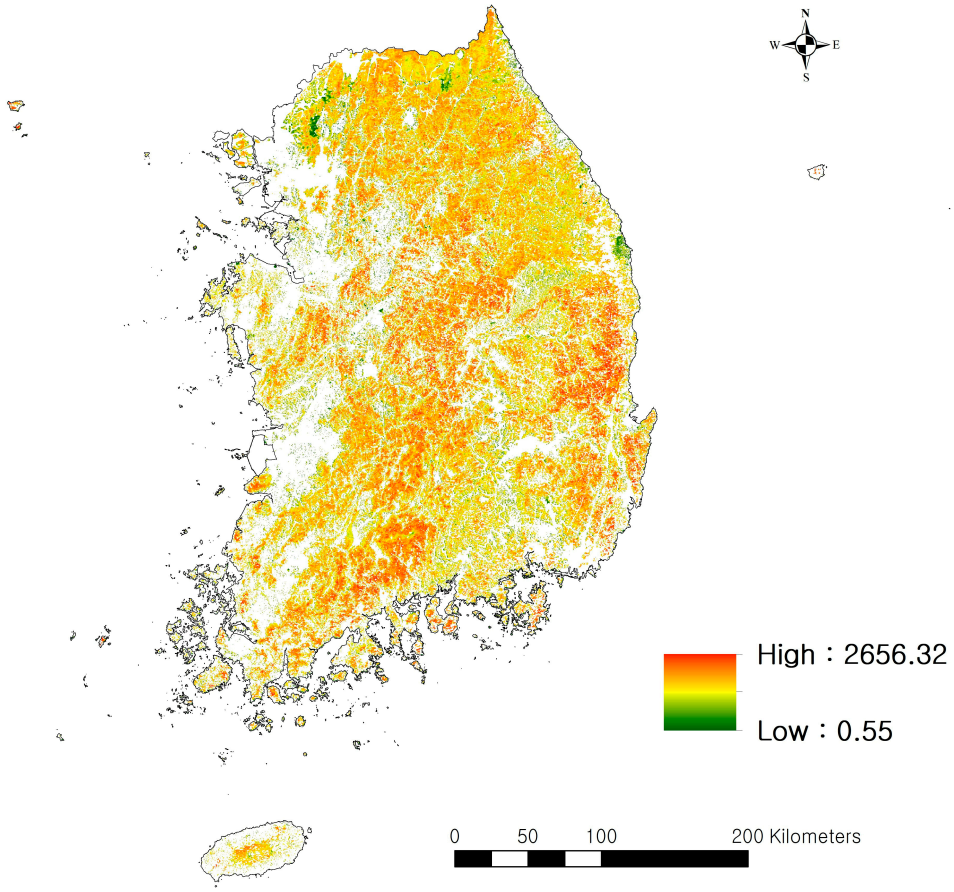


Figure 2. Spatial distribution of net primary productivity (NPP) across South Korea in 2024, estimated using the CASA model.

3.2. Net Ecosystem Production (NEP)

Total NEP in 2024 was 63.29 Mt CO_2 yr^{-1}. Widespread positive NEP (net carbon sinks) occurred along the Baekdudaegan Range and the Yeongnam Alps, with extensive areas exceeding 8 t CO_2 ha^{-1} yr^{-1} (Figure 4). In contrast, lowland regions dominated by urban development or intensive agriculture showed markedly lower NEP. Localized negative NEP pockets are evident where RH exceeds NPP, indicating net carbon emissions from terrestrial ecosystems.

3.3. Heterotrophic Respiration (RH)

The national total RH in 2024 was 15.35 Mt CO_2 yr^{-1}. Per-area RH values ranged from 8.36 to 13.96 t CO_2 ha^{-1} yr^{-1}, with elevated levels in warm, humid lowlands and coastal plains of the western and southern provinces (Figure 3). Lower RH characterizes high-elevation forests in eastern Gangwon-do and the uplands of Jeju Island. Where urban pixels were excluded from analysis, they are treated as masked (not evaluated) rather than low-value areas, consistent with sealed surfaces and limited organic substrates.

3.4. Temporal Changes in NPP

From 2010 to 2024, spatially averaged NPP varied between 1170 and 1543 g C m^{-2} yr^{-1}, showing an overall upward tendency (Figure 5). Annual totals ranged from 47.34 to 78.63 Mt CO_2 yr^{-1} after correcting an internal transcription error in 2018 (Figure 5). Differences between mean and total NPP in specific years (e.g., 2012, 2016) are attributable to variations in effective vegetated area and updates to masking (e.g., data

gaps, cloud/snow screening) and land-cover classification (see Methods Section 2.3.5 for compositing and masking procedures).

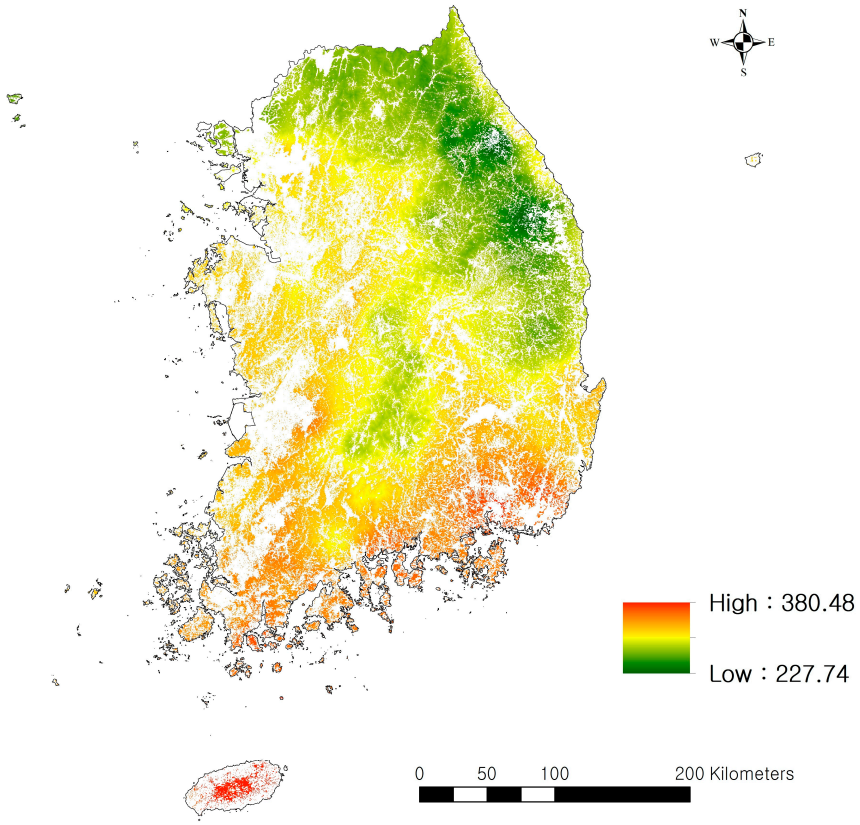


Figure 3. Spatial distribution of heterotrophic respiration (RH) across South Korea in 2024.

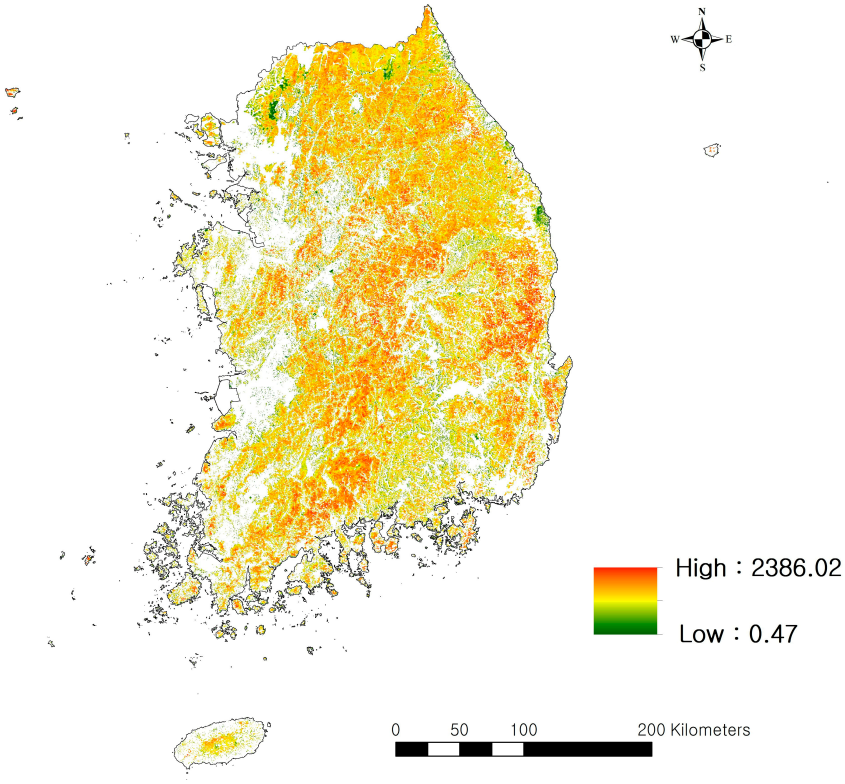


Figure 4. Spatial distribution of net ecosystem production (NEP) across South Korea in 2024.

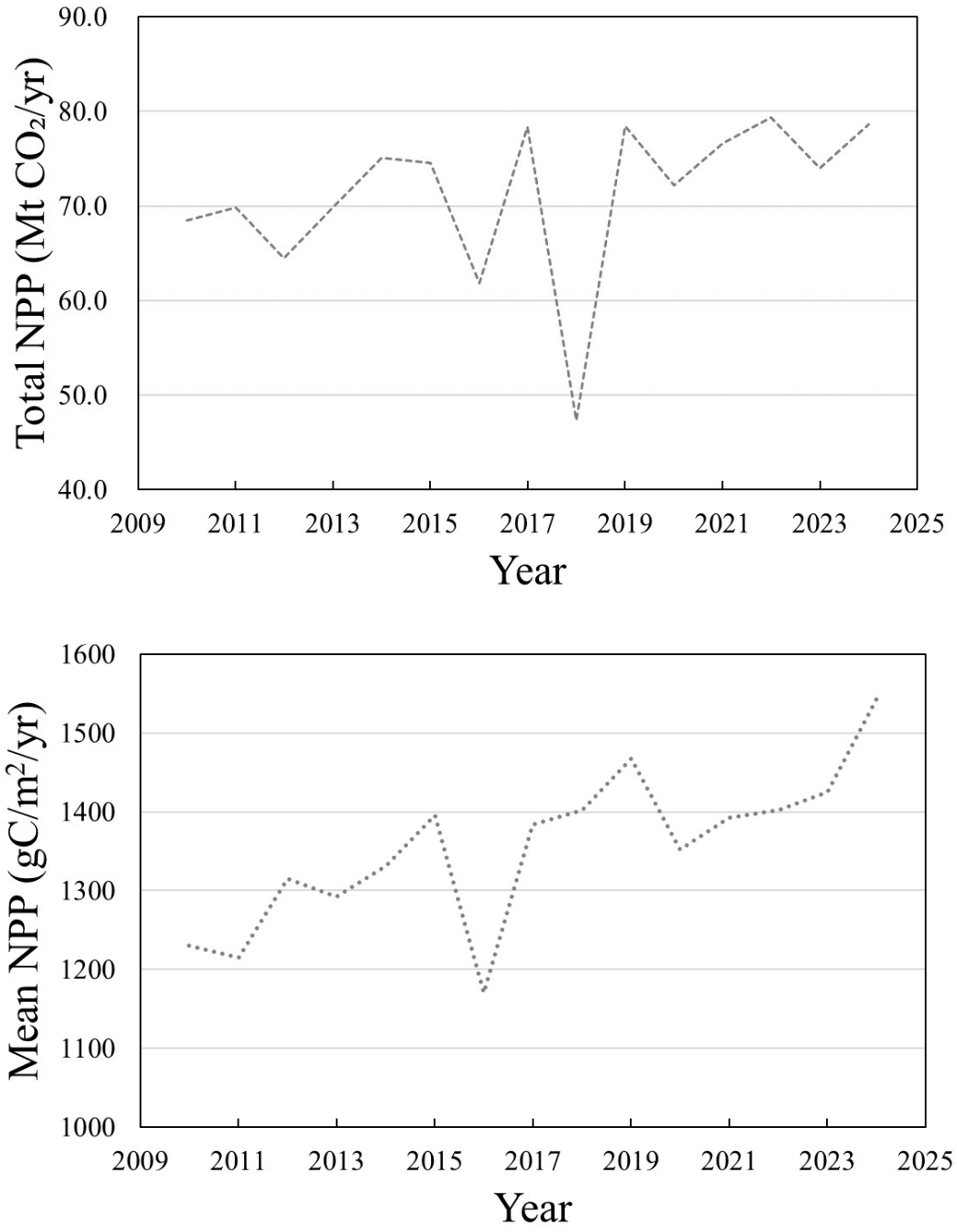


Figure 5. The temporal trends in the total (**upper**) and mean (**lower**) NPP (Mt $CO_2 yr^{-1}$) over 15 years from 2010 to 2024 in South Korea.

4. Discussion

4.1. Accuracy and Representativeness of the Estimated NEP

Our NEP fields inherit fidelity from their two constituent fluxes, NPP and RH. NPP was generated using a CASA-type LUE framework, in which APAR is derived from shortwave radiation and FPAR, while ε is down-regulated by temperature and water scalars relative to a biome-specific ε_{max} [22]. Cross-biome and regional evaluations indicate that model performance improves with optimized meteorological inputs, high-resolution land cover, and evapotranspiration (ET) constraints, and that mid- to high-relief settings particularly benefit from finer spatial detail or data fusion [31,43,46,47]. Applications across East Asia, including Korea's complex landscapes, show good agreement with flux and plot benchmarks as well as realistic interannual variability [41,48,49]. Recent advances, such as

improved scalar formulations and orographic adaptations, further support use in mountain vegetation [32], while large-area implementations via cloud platforms demonstrate scalability [27,28].

RH was estimated with a climate-response function based on temperature and precipitation. While pragmatic at the national scale, soil respiration exhibits strong interannual variability and edaphic controls that climate-only predictors may not capture [50]. Site-level evidence from Korean forests indicates substantial annual respiration, suggesting that local RH may exceed simple climate-based expectations where substrates and microbial activity are high [18,51].

To minimize arithmetic and scaling errors, we enforced unit harmonization (g C m^{-2} yr^{-1} ↔ t CO_2 ha^{-1} yr^{-1}) and cross-checked annual means against totals. After resolving an outlier year, national NEP statistics and maps were produced with consistent units.

Comparing the estimated NEP with the field-measured NEP also confirmed the representativeness of the value. The national-scale NEP was estimated at approximately 63.3 Mt CO_2 yr^{-1}, which was similar to values measured in the field. For example, Lee et al. [52] estimated carbon stock as 60,648 Gg CO_2 per year and Kim et al. [35] estimated carbon sequestration potential calculated based on NEP derived from the difference between NPP and HR estimated as 70.3 Mt CO_2 yr^{-1}.

4.2. Spatiotemporal Variability of NEP

The spatial and temporal variability of NEP in this study reflected the combined influence of vegetation type, topography, and climate drivers. The spatial distribution analysis (Figure 3) revealed that mountainous regions exhibited higher NEP values compared with lowland and urban areas, including the Baekdudaegan range and the northern mountains of Gyeongsangbuk-do, which recorded the highest NEP values, frequently exceeding 8.0 t CO_2 ha^{-1} yr^{-1}. This pattern is attributed to dense forest cover, low anthropogenic disturbance, and relatively low RH. These results are consistent with Long et al. [53], who reported that forest-dominated regions in East Asia sustain elevated NEP due to persistent canopy productivity and reduced human pressure.

In contrast, urban centers and low-lying agricultural zones, particularly in the western and southern coastal areas, exhibited NEP values below 2.0 t CO_2 ha^{-1} yr^{-1}. In some grid cells, NEP was negative because RH exceeded NPP. Zhang and Liu [1] emphasized that land-use intensification and impervious surface expansion in peri-urban landscapes markedly reduce ecosystem productivity, reinforcing the patterns observed in this study.

The spatial distribution of these NEPs showed a similar pattern to the spatial distribution prepared based on the data measured in the field [35], and the spatial distribution trend of RH also showed a similar trend to the results measured in the field [51]. In this regard, the reliability of the results obtained through this study could be confirmed.

Temporally, interannual variation in NEP was driven largely by fluctuations in NDVI, temperature, and precipitation. The lowest national NEP (47.3 Mt CO_2) occurred in 2018, coinciding with a decline in spring temperatures and intensified summer rainfall, both of which constrained NPP. This finding corroborates the climate sensitivity highlighted by Xu et al. [29], who showed that vegetation productivity in East Asian uplands is particularly vulnerable to seasonal climatic anomalies. Conversely, 2024 recorded the highest NEP (78.6 Mt CO_2), reflecting both an increase in mean NPP and an expansion of high-productivity vegetation cover.

Taken together, these results indicate that NEP is a dynamic indicator shaped by land use and climate variability, and that it is especially responsive to temperature-driven photosynthetic activity, consistent with established observations across East Asia.

4.3. Relationship Between NEP and Climate and Vegetation Factors

The spatial and temporal variation in NEP observed in this study reflects the coupled influence of climatic conditions and vegetation characteristics on both carbon absorption and emission processes. Because NEP is derived from the difference between NPP and RH [36], its variability is inherently sensitive to the environmental drivers of these components [54–56].

Vegetation greenness, represented by the Normalized Difference Vegetation Index (NDVI), is a central input in the CASA model and strongly correlates with NPP. NDVI integrates canopy structure and chlorophyll content, and it responds to interannual and seasonal changes in photosynthetic activity. Zhao and Running [57] demonstrated that global reductions in NPP during drought episodes were largely attributable to suppressed NDVI and reduced evapotranspiration (ET), underscoring NDVI's role as a diagnostic proxy for vegetation productivity. Consistent with this, NEP in our study was highest in years such as 2020 and 2024, coinciding with elevated NDVI and above-average temperatures.

Temperature is another major determinant of both NPP and RH. Moderate warming can enhance photosynthetic rates, particularly in temperate and boreal ecosystems, whereas excessive warming may disproportionately accelerate RH through enhanced microbial decomposition [51]. Reichstein et al. [58], analyzing European eddy-covariance data, showed that temperature and water availability jointly regulate the ecosystem carbon balance, with drought and heat stress reducing NEP primarily through elevated respiration. Similarly, Law et al. [59] demonstrated that forest carbon and water vapor exchanges are strongly influenced by vapor-pressure deficit, temperature, and soil moisture—drivers that are also incorporated into the empirical RH estimation applied in this study.

Vegetation type further modulates these responses. Forests, particularly at higher elevations, generally exhibit higher light-use efficiency (ε_{max}) and greater carbon sequestration capacity than croplands or urban vegetation. Consistent with this, our maps show that forest-dense mountainous zones record the highest NEP, whereas low-lying agricultural and urbanized areas exhibit substantially lower, and in some cases negative, values. This spatial heterogeneity in NEP is consistent with the patterns reported by Jung et al. [60], who identified forest biomes as persistent net carbon sinks globally, in contrast to managed landscapes characterized by lower productivity and faster carbon turnover.

Overall, NEP is shaped by complex, non-linear interactions among canopy greenness (NDVI), air temperature, precipitation, vapor-pressure deficit, and vegetation structure [42]. These findings highlight the need for integrative modeling approaches that account for both spatial heterogeneity and climatic anomalies. Accordingly, NEP serves as a sensitive indicator of ecosystem responses to natural variability and anthropogenic land-use change [54–56].

4.4. Limitations and Future Directions

4.4.1. Limitations of the CASA Approach

The evaluation of carbon sequestration potential using the Carnegie–Ames–Stanford Approach (CASA) model has provided valuable insights into ecosystem productivity and carbon dynamics at regional and global scales. However, several limitations must be acknowledged to interpret the results accurately and to improve future applications. At the same time, emerging opportunities in remote sensing, data integration, and process modeling offer promising directions for enhancing CASA-based assessments.

A primary limitation of the CASA model lies in its strong dependence on remote sensing-derived vegetation indices, particularly the Normalized Difference Vegetation Index (NDVI). Although NDVI serves as a robust proxy for canopy greenness, it tends to saturate in high-biomass regions such as dense forests and is sensitive to atmospheric

interference from aerosols and clouds. Consequently, this can lead to biased estimates of absorbed photosynthetically active radiation (APAR) and, subsequently, net primary productivity (NPP). In addition, CASA often utilizes Moderate Resolution Imaging Spectroradiometer (MODIS) data at 500 m to 1 km spatial resolution, which may not capture fine-scale heterogeneity in fragmented landscapes, urban–forest mosaics, or agricultural systems [61,62]

Another limitation is the model's simplified representation of ecosystem processes. CASA employs a light-use efficiency (LUE) framework in which NPP is calculated as the product of APAR and biome-specific maximum efficiency (ε_{max}), modulated by stress scalars for temperature and moisture. However, this formulation does not explicitly account for critical constraints such as nutrient availability (e.g., nitrogen and phosphorus), soil–microbial interactions, or CO_2 fertilization effects. The assumption of static biome-level ε_{max} values further introduces uncertainty, as it neglects local adaptations and management practices that significantly influence productivity [31,50,63].

Uncertainty in climate input data is another major source of error. CASA relies on temperature, precipitation, and solar radiation datasets, which are often derived from reanalysis products or interpolated weather observations. Errors or biases in these inputs can propagate through the model, affecting productivity estimates. Moreover, CASA does not explicitly simulate the impacts of extreme events such as droughts, heatwaves, or typhoons beyond their averaged influence on NDVI and climate stress scalars, leading to an underestimation of variability in carbon fluxes during anomalous periods [64,65].

The estimation of net ecosystem production (NEP) introduces additional challenges. While CASA provides relatively robust estimates of NPP, NEP requires the subtraction of heterotrophic respiration (RH), which is frequently derived from empirical regressions rather than mechanistic soil carbon models. This approach limits the ability to capture spatial and temporal variability in soil decomposition dynamics, particularly under changing climate conditions. Similarly, disturbances such as wildfires, insect outbreaks, and land-use changes are not explicitly represented, potentially biasing carbon sink assessments [49,66,67].

Validation also remains a critical bottleneck. Ground-based flux measurements from eddy covariance towers are sparse and unevenly distributed, especially in mountainous, boreal, or urbanized regions. This scarcity hampers efforts to rigorously evaluate CASA outputs at regional scales. Furthermore, inventory-based biomass datasets and long-term ecological monitoring plots are not consistently integrated with CASA estimates, resulting in limited cross-validation between remote sensing–based and field-based carbon assessments [68,69].

4.4.2. Future Directions for Improvement

To address these limitations, future applications of CASA should focus on integrating higher-resolution and multi-source remote sensing data. Incorporating Sentinel-2 and Landsat time series can enhance spatial detail in heterogeneous landscapes, while combining NDVI with alternative vegetation indices (e.g., Enhanced Vegetation Index, EVI) and solar-induced chlorophyll fluorescence (SIF) can improve estimates of photosynthetic activity. These enhancements can reduce biases associated with NDVI saturation and better capture short-term physiological responses [70–72].

Dynamic parameterization represents another key avenue for refinement. Instead of relying on static biome-level ε_{max} values, CASA could employ region-specific or temporally varying efficiency parameters calibrated using flux tower observations and inventory data. Emerging machine learning techniques offer additional opportunities for adaptive parameter optimization across diverse ecosystems and climate regimes [73].

Coupling CASA with process-based biogeochemical models such as CENTURY or DAYCENT holds significant potential for improving soil carbon dynamics and RH estimation. Such integration would enable the explicit representation of nutrient cycling, soil moisture variability, and decomposition processes, thereby reducing uncertainty in NEP calculations. Additionally, incorporating drought indices (e.g., Standardized Precipitation–Evapotranspiration Index) and heat stress thresholds into CASA stress scalars would allow for a better characterization of extreme events, which are increasingly important under climate change scenarios. Similarly, incorporating disturbance modules for fire, pests, and land-use change—based on satellite-derived disturbance datasets—would improve the accuracy of long-term carbon sink projections [74,75].

Uncertainty quantification should become an integral component of CASA-based studies. Developing frameworks to propagate errors from input datasets, model parameters, and RH estimates would enhance the reliability and transparency of carbon assessments. Data assimilation techniques, including Bayesian calibration, could further constrain model outputs by integrating observational data such as eddy covariance fluxes, inventory-based biomass measurements, and forest growth plots.

Finally, the application of CASA should increasingly align with policy-oriented frameworks for carbon neutrality and climate mitigation. Linking CASA outputs with national greenhouse gas inventories under Intergovernmental Panel on Climate Change (IPCC) Tier 2 or Tier 3 methodologies can provide more consistent and verifiable estimates of land-based carbon sequestration. Furthermore, developing decision-support tools that incorporate CASA outputs into nature-based solutions (NbSs) planning and carbon offset verification can facilitate their integration into corporate and national climate strategies [19,33].

4.4.3. Implications for Climate Policy and Carbon Neutrality

Enhancing the CASA model and its integration with complementary data and process-based approaches is critical for supporting carbon neutrality targets and evidence-based climate policy. The accurate assessment of ecosystem carbon sequestration potential underpins national greenhouse gas inventories, land-use planning, and the design of nature-based solutions for climate mitigation. By improving spatial resolution, dynamic parameterization, and disturbance representation, CASA can provide more robust estimates that are suitable for compliance with IPCC reporting guidelines and carbon market verification. Ultimately, advancing CASA-based assessments will not only strengthen the scientific understanding of terrestrial carbon dynamics, but also enable policymakers and stakeholders to implement more effective strategies for achieving net-zero emissions [67,71].

5. Conclusions

This study presents a flux-based, unit-harmonized assessment of terrestrial carbon exchange across South Korea, applying a CASA-type framework for NPP and a climate-response model for heterotrophic respiration (RH).

Spatial patterns are robust and physically interpretable: forest-dense uplands—particularly along the Baekdudaegan Range, around Mt. Jirisan, and in the northern mountains of Gyeongsangbuk-do—function as strong carbon sinks, frequently exceeding 8 t CO_2 ha^{-1} yr^{-1}. By contrast, low-lying agro-urban corridors, including the Seoul Metropolitan Area and coastal plains such as Jeollanam-do and the Nakdong River basin, exhibit much lower and in some cases, negative NEP. These contrasts reflect co-variation in canopy greenness (FPAR/NDVI), thermal and moisture scalars, and land cover.

Temporally, the 2010–2024 period shows pronounced interannual variability alongside an overall upward tendency in spatially averaged NPP, consistent with climate-driven modulation of productivity. Discrepancies between annual means and totals in certain

years (e.g., 2018) were traced to effective vegetated-area and masking differences and were corrected to preserve the internal coherence of the time series.

Methodologically, the integration of satellite-driven NPP with an empirical RH response enabled wall-to-wall mapping at 250 m resolution, with transparent assumptions and repeatable processing. At the same time, the results highlight the need to refine RH estimation where substrate and microbial controls are strong and to mitigate mixed-pixel effects in mosaicked landscapes. These priorities point toward the future integration of high-resolution optical and microwave products, soil datasets, and local calibration of ε_{max} and scalar responses against Korean flux towers.

Taken together, the finalized NEP maps and statistics provide a consistent national baseline for carbon budgeting, ecosystem monitoring, and land-based mitigation planning. Because NEP responds sensitively to climate anomalies and land-use intensity, the framework presented here is well-suited for tracking policy outcomes and for near-real-time surveillance of ecosystem carbon balance under ongoing environmental change.

While CASA provides an effective framework for large-scale carbon assessment, limitations remain regarding the accuracy and representativeness of NEP estimates, particularly due to reliance on NDVI, simplified respiration modeling, and the exclusion of disturbance effects. Future improvements should include higher-resolution remote sensing, dynamic parameterization, and coupling with process-based models to better capture nutrient dynamics, soil moisture variability, and extreme events. These refinements, alongside rigorous ground-based validation, will enhance the reliability of CASA outputs for supporting carbon neutrality policies.

In conclusion, South Korea's terrestrial ecosystems act as a significant carbon sink, with forested uplands playing a critical role in offsetting national emissions. Improving CASA-based modeling approaches will be essential for accurately quantifying land-based carbon sequestration and informing climate strategies aligned with IPCC guidelines and net-zero commitments.

Author Contributions: Conceptualization, C.-S.L. and N.-S.K.; methodology, J.-H.L.; software, N.-S.K.; validation, N.-S.K., J.-H.L. and C.-S.L.; formal analysis, N.-S.K. and J.-H.L.; investigation, C.-S.L.; resources, N.-S.K.; data curation, N.-S.K.; writing—original draft preparation, N.-S.K.; writing—review and editing, C.-S.L.; visualization, J.-H.L.; supervision, C.-S.L.; project administration, C.-S.L.; funding acquisition, N.-S.K. All authors have read and agreed to the published version of the manuscript.

Funding: This research was initially funded by the Ministry of Environment (MOE) and the National Institute of Ecology (NIE), Rep. of Korea (Project No. NIE-C-2025-19 and NIE-B-2025-03).

Institutional Review Board Statement: Not applicable.

Informed Consent Statement: Not applicable.

Data Availability Statement: The data presented in this study are available on request from the corresponding author.

Conflicts of Interest: The authors declare no conflicts of interest.

Abbreviations

The following abbreviations are used in this manuscript:

NPP	Net Primary Productivity
HR	Heterotrophic Respiration
NEP	Net Ecosystem Production

References

1. Zhang, C.; Liu, J. The Impact of Land-Use Changes on the Spatiotemporal Dynamics of Net Primary Productivity in Harbin, China. *Sustainability* **2025**, *17*, 5979. [CrossRef]
2. Wang, F.; Harindintwali, J.D.; Yuan, Z.; Wang, M.; Wang, F.; Li, S.; Yin, Z.; Huang, L.; Fu, Y.; Li, L.; et al. Technologies and Perspectives for Achieving Carbon Neutrality. *Innovation* **2021**, *2*, 100180. [CrossRef]
3. Chen, C.; Haupert, S.R.; Zimmermann, L.; Shi, X.; Fritsche, L.G.; Mukherjee, B. Global Prevalence of Post-Coronavirus Disease 2019 (COVID-19) Condition or Long COVID: A Meta-Analysis and Systematic Review. *J. Infect. Dis.* **2022**, *226*, 1593–1607. [CrossRef] [PubMed]
4. Al Khaffaf, I.; Tamimi, A.; Ahmed, V. Pathways to Carbon Neutrality: A Review of Strategies and Technologies Across Sectors. *Energies* **2024**, *17*, 6129. [CrossRef]
5. Höhne, N.; Gidden, M.J.; den Elzen, M.; Hans, F.; Fyson, C.; Geiges, A.; Jeffery, M.L.; Gonzales-Zuñiga, S.; Mooldijk, S.; Hare, W.; et al. Wave of Net Zero Emission Targets Opens Window to Meeting the Paris Agreement. *Nat. Clim. Change* **2021**, *11*, 820–822. [CrossRef]
6. Fankhauser, S.; Smith, S.M.; Allen, M.; Axelsson, K.; Hale, T.; Hepburn, C.; Kendall, J.M.; Khosla, R.; Lezaun, J.; Mitchell-Larson, E.; et al. The Meaning of Net Zero and How to Get It Right. *Nat. Clim. Change* **2022**, *12*, 15–21. [CrossRef]
7. Rogelj, J. Net Zero Targets in Science and Policy. *Environ. Res. Lett.* **2023**, *18*, 021003. [CrossRef]
8. Davis, S.J.; Lewis, N.S.; Shaner, M.; Aggarwal, S.; Arent, D.; Azevedo, I.L.; Benson, S.M.; Bradley, T.; Brouwer, J.; Chiang, Y.-M.; et al. Net-Zero Emissions Energy Systems. *Science* **2018**, *360*, eaas9793. [CrossRef]
9. Minx, J.C.; Lamb, W.F.; Callaghan, M.W.; Fuss, S.; Hilaire, J.; Creutzig, F.; Amann, T.; Beringer, T.; Garcia, W.d.O.; Hartmann, J.; et al. Negative Emissions—Part 1: Research Landscape and Synthesis. *Environ. Res. Lett.* **2018**, *13*, 063001. [CrossRef]
10. Griscom, B.W.; Adams, J.; Ellis, P.W.; Houghton, R.A.; Lomax, G.; Miteva, D.A.; Schlesinger, W.H.; Shoch, D.; Siikamäki, J.V.; Smith, P.; et al. Natural Climate Solutions. *Proc. Natl. Acad. Sci. USA* **2017**, *114*, 11645–11650. [CrossRef]
11. Seddon, N.; Chausson, A.; Berry, P.; Girardin, C.A.J.; Smith, A.; Turner, B. Understanding the Value and Limits of Nature-Based Solutions to Climate Change and Other Global Challenges. *Philos. Trans. R. Soc. B Biol. Sci.* **2020**, *375*, 20190120. [CrossRef]
12. Chausson, A.; Turner, B.; Seddon, D.; Chabaneix, N.; Girardin, C.A.J.; Kapos, V.; Key, I.; Roe, D.; Smith, A.; Woroniecki, S.; et al. Global Change Biology | Environmental Change Journal | Wiley Online Library. Available online: https://onlinelibrary.wiley.com/doi/10.1111/gcb.15310 (accessed on 12 September 2025).
13. Pan, Y.; Birdsey, R.A.; Fang, J.; Houghton, R.; Kauppi, P.E.; Kurz, W.A.; Phillips, O.L.; Shvidenko, A.; Lewis, S.L.; Canadell, J.G.; et al. A Large and Persistent Carbon Sink in the World's Forests Science. Available online: https://www.science.org/doi/10.1126/science.1201609 (accessed on 12 September 2025).
14. Friedlingstein, P.; O'Sullivan, M.; Jones, M.W.; Andrew, R.M.; Hauck, J.; Landschützer, P.; Quéré, C.L.; Li, H.; Luijkx, I.T.; Olsen, A.; et al. ESSD—Global Carbon Budget 2024. Available online: https://essd.copernicus.org/articles/17/965/2025/ (accessed on 12 September 2025).
15. Bui, M.; Adjiman, C.S.; Bardow, A.; Boston, A.; Brown, S.; Fennell, P.S.; Fuss, S.; Galindo, A.; Hacketti, L.A.; Hallett, J.P.; et al. Carbon Capture and Storage (CCS): The Way Forward. *Energy Environ. Sci.* **2018**, *11*, 1062–1176. [CrossRef]
16. van der Ploeg, R.; Haigh, M. The Importance of Natural Land Carbon Sinks in Modelling Future Emissions Pathways and Assessing Individual Country Progress towards Net-Zero Emissions Targets. *Front. Environ. Sci.* **2024**, *12*, 1379046. [CrossRef]
17. Grassi, G.; Stehfest, E.; Rogelj, J.; van Vuuren, D.; Cescatti, A.; House, J.; Nabuurs, G.-J.; Rossi, S.; Alkama, R.; Viñas, R.A.; et al. Critical Adjustment of Land Mitigation Pathways for Assessing Countries' Climate Progress | Nature Climate Change. Available online: https://www.nature.com/articles/s41558-021-01033-6 (accessed on 12 September 2025).
18. Lim, B.-S.; Joo, S.-J.; Seok, J.-E.; Lee, C.-S. An Assessment of the Carbon Budget of the Passively Restored Willow Forests Along the Miho River, Central South Korea. *Climate* **2024**, *12*, 182. [CrossRef]
19. Chen, H.; Wei, Y.; Huang, J.J. Urbanization Diminishes Net Ecosystem Productivity by Changing the Landscape Pattern. *Agric. For. Meteorol.* **2025**, *362*, 110369. [CrossRef]
20. Lyu, J.; Fu, X.; Lu, C.; Zhang, Y.; Luo, P.; Guo, P.; Huo, A.; Zhou, M. Quantitative Assessment of Spatiotemporal Dynamics in Vegetation NPP, NEP and Carbon Sink Capacity in the Weihe River Basin from 2001 to 2020. *J. Clean. Prod.* **2023**, *428*, 139384. [CrossRef]
21. Houghton, R.A. Revised Estimates of the Annual Net Flux of Carbon to the Atmosphere from Changes in Land Use and Land Management 1850–2000. *Tellus B Chem. Phys. Meteorol.* **2003**, *55*, 378–390.
22. Potter, C.S.; Randerson, J.T.; Field, C.B.; Matson, P.A.; Vitousek, P.M.; Mooney, H.A.; Klooster, S.A. Terrestrial Ecosystem Production: A Process Model Based on Global Satellite and Surface Data. *Glob. Biogeochem. Cycles* **1993**, *7*, 811–841. [CrossRef]
23. Zhao, M.; Heinsch, F.A.; Nemani, R.R.; Running, S.W. Improvements of the MODIS Terrestrial Gross and Net Primary Production Global Data Set. *Remote Sens. Environ.* **2005**, *95*, 164–176. [CrossRef]
24. Yuan, W.; Xia, J.; Song, C.; Wang, Y.-P. Simulating the Land Carbon Sink: Progresses and Challenges of Terrestrial Ecosystem Models. *Agric. For. Meteorol.* **2024**, *358*, 110264. [CrossRef]

25. Fuller, M.R.; Ganjam, M.; Baker, J.S.; Abt, R.C. Advancing Forest Carbon Projections Requires Improved Convergence between Ecological and Economic Models. *Carbon Balance Manag.* **2025**, *20*, 2. [CrossRef] [PubMed]
26. Huang, Z.; Li, X.; Mao, F.; Huang, L.; Zhao, Y.; Song, M.; Yu, J.; Du, H. Integrating LUCC and Forest Aging to Project and Attribute Subtropical Forest NEP in Zhejiang Province under Four SSP-RCP Scenarios. *Agric. For. Meteorol.* **2025**, *365*, 110462. [CrossRef]
27. Dong, D.; Zhang, R.; Guo, W.; Gong, D.; Zhao, Z.; Zhou, Y.; Xu, Y.; Fujioka, Y. Assessing Spatiotemporal Dynamics of Net Primary Productivity in Shandong Province, China (2001–2020) Using the CASA Model and Google Earth Engine: Trends, Patterns, and Driving Factors. *Remote Sens.* **2025**, *17*, 488. [CrossRef]
28. Yisilayili, G.; He, B.; Song, Y.; Luo, X.; Yang, W.; Chen, Y. Simulation of Vegetation NPP in Typical Arid Regions Based on the CASA Model and Quantification of Its Driving Factors. *Land* **2025**, *14*, 371. [CrossRef]
29. Xu, H.; He, B.; Guo, L.; Yan, X.; Zeng, Y.; Yuan, W.; Zhong, Z.; Tang, R.; Yang, Y.; Liu, H. Global Forest Plantations Mapping and Biomass Carbon Estimation. *J. Geophys. Res. Biogeosciences* **2024**, *129*, e2023JG007441. [CrossRef]
30. Intergovernmental Panel on Climate Change (IPCC). *2006 IPCC Guidelines for National Greenhouse Gas Inventories*; IUCN: Gland, Switzerland, 2006.
31. Jay, S.; Potter, C.; Crabtree, R.; Genovese, V.; Weiss, D.J.; Kraft, M. Evaluation of Modelled Net Primary Production Using MODIS and Landsat Satellite Data Fusion. *Carbon Balance Manag.* **2016**, *11*, 8. [CrossRef]
32. Huang, X.; He, L.; He, Z.; Nan, X.; Lyu, P.; Ye, H. An Improved Carnegie-Ames-Stanford Approach Model for Estimating Ecological Carbon Sequestration in Mountain Vegetation. *Front. Ecol. Evol.* **2022**, *10*, 1048607. [CrossRef]
33. Zhang, L.; Li, M.; Zhang, Z.; Li, L.; Yuan, J.; Zhu, S.; Wang, H.; Jia, M.; Ruan, J.; Pang, L.; et al. Aligning Regional Carbon Neutrality Pathways with National Climate Goals: An Integrated Analytical Framework. *Environ. Sci. Ecotechnology* **2025**, *25*, 100571. [CrossRef]
34. Liu, Y.; Xia, C.; Ou, X.; Lv, Y.; Ai, X.; Pan, R.; Zhang, Y.; Shi, M.; Zheng, X. Quantitative Structure and Spatial Pattern Optimization of Urban Green Space from the Perspective of Carbon Balance: A Case Study in Beijing, China. *Ecol. Indic.* **2023**, *148*, 110034. [CrossRef]
35. Kim, G.S.; Kim, A.R.; Lim, B.S.; Seol, J.; An, J.H.; Lim, C.H.; Joo, S.J.; Lee, C.S. Assessment of the Carbon Budget of Local Governments in South Korea. *Atmosphere* **2022**, *13*, 342. [CrossRef]
36. Goovaerts, P. Geostatistical Approaches for Incorporating Elevation into the Spatial Interpolation of Rainfall. *J. Hydrol.* **2000**, *228*, 113–129. [CrossRef]
37. Lloyd, C. Assessing the Effect of Integrating Elevation Data into the Estimation of Monthly Precipitation in Great Britain. *J. Hydrol.* **2005**, *308*, 128–150. [CrossRef]
38. Turner, D.P.; Ritts, W.D.; Cohen, W.B.; Gower, S.T.; Running, S.W.; Zhao, M.; Costa, M.H.; Kirschbaum, A.A.; Ham, J.M.; Saleska, S.R.; et al. Evaluation of MODIS NPP and GPP Products across Multiple Biomes. *Remote Sens. Environ.* **2006**, *102*, 282–292. [CrossRef]
39. Yuan, W.; Liu, S.; Zhou, G.; Zhou, G.; Tieszen, L.L.; Baldocchi, D.; Bernhofer, C.; Gholz, H.; Goldstein, A.H.; Goulden, M.L.; et al. Deriving a Light Use Efficiency Model from Eddy Covariance Flux Data for Predicting Daily Gross Primary Production across Biomes. *Agric. For. Meteorol.* **2007**, *143*, 189–207. [CrossRef]
40. Sasai, T.; Saigusa, N.; Nasahara, K.N.; Ito, A.; Hashimoto, H.; Nemani, R.; Hirata, R.; Ichii, K.; Takagi, K.; Saitoh, T.M.; et al. Satellite-Driven Estimation of Terrestrial Carbon Flux over Far East Asia with 1-Km Grid Resolution. *Remote Sens. Environ.* **2011**, *115*, 1758–1771. [CrossRef]
41. Shim, C.; Hong, J.; Hong, J.; Kim, Y.; Kang, M.; Thakuri, B.M.; Kim, Y.; Chun, J. Evaluation of MODIS GPP over a Complex Ecosystem in East Asia: A Case Study at Gwangneung Flux Tower in Korea. *Adv. Space Res.* **2014**, *54*, 2296–2308. [CrossRef]
42. Didan, K. MYD13A1 MODIS/Aqua Vegetation Indices 16-Day L3 Global 500m SIN Grid V006. NASA EOSDIS Land Processes Distributed Active Archive Center (DAAC) Data Set. MYD13A1-006. 2015. Available online: https://www.earthdata.nasa.gov/data/catalog/lpcloud-myd13a1-006 (accessed on 12 October 2025).
43. Mu, Q.; Zhao, M.; Running, S.W. Improvements to a MODIS Global Terrestrial Evapotranspiration Algorithm. *Remote Sens. Environ.* **2011**, *115*, 1781–1800. [CrossRef]
44. Raich, J.W.; Potter, C.S. Global Patterns of Carbon Dioxide Emissions from Soils. *Glob. Biogeochem. Cycles* **1995**, *9*, 23–36. [CrossRef]
45. Bond-Lamberty, B.; Thomson, A. Temperature-Associated Increases in the Global Soil Respiration Record | Nature. Available online: https://www.nature.com/articles/nature08930 (accessed on 12 September 2025).
46. Turner, D.P.; Urbanski, S.; Bremer, D.; Wofsy, S.C.; Meyers, T.; Gower, S.T.; Gregory, M. A Cross-Biome Comparison of Daily Light Use Efficiency for Gross Primary Production. *Glob. Change Biol.* **2003**, *9*, 383–395. [CrossRef]
47. Park, H.; Im, J.; Kim, M. Improvement of Satellite-Based Estimation of Gross Primary Production through Optimization of Meteorological Parameters and High Resolution Land Cover Information at Regional Scale over East Asia. *Agric. For. Meteorol.* **2019**, *271*, 180–192. [CrossRef]
48. Hwang, K.; Choi, M. Seasonal Trends of Satellite-Based Evapotranspiration Algorithms over a Complex Ecosystem in East Asia. *Remote Sens. Environ.* **2013**, *137*, 244–263. [CrossRef]

49. Wang, P.; Xue, Y.; Yan, Z.; Yin, W.; He, B.; Li, P. Study of Regional Spatial and Temporal Changes of Net Ecosystem Productivity of Crops from Remotely Sensed Data. *Land* **2024**, *13*, 155. [CrossRef]
50. Raich, J.W.; Potter, C.S.; Bhagawati, D. Interannual Variability in Global Soil Respiration, 1980–1994. *Glob. Change Biol.* **2002**, *8*, 800–812. [CrossRef]
51. Kim, G.S.; Joo, S.J.; Lee, C.S. Seasonal Variation of Soil Respiration in the Mongolian Oak (Quercus Mongolica Fisch. Ex Ledeb.) Forests at the Cool Temperate Zone in Korea. *Forests* **2020**, *11*, 984. [CrossRef]
52. Lee, S.J.; Yim, J.S.; Son, Y.M.; Son, Y.; Kim, R. Estimation of Forest Carbon Stocks for National Greenhouse Gas Inventory Reporting in South Korea. *Forests* **2018**, *9*, 625. [CrossRef]
53. Long, T.; Wang, Y.; Jiang, Y.; Zhang, Y.; Wang, B. Spatiotemporal Evolution and Driving Factors of NPP in the LanXi Urban Agglomeration from 2000 to 2023. *Sustainability* **2025**, *17*, 5804. [CrossRef]
54. Moustakis, Y.; Fatichi, S.; Onof, C.; Paschalis, A. Insensitivity of Ecosystem Productivity to Predicted Changes in Fine-Scale Rainfall Variability. *J. Geophys. Res. Biogeosciences* **2022**, *127*, e2021JG006735. [CrossRef]
55. Xiao, J.; Wang, Z.; Sun, W.; Li, S.; Han, F.; Huang, S.; Yu, C. The Relative Effects of Climate Change and Phenological Change on Net Primary Productivity Vary with Grassland Types on the Tibetan Plateau. *Remote Sens.* **2023**, *15*, 3733. [CrossRef]
56. Ryan-Keogh, T.J.; Tagliabue, A.; Thomalla, S.J. Global Decline in Net Primary Production Underestimated by Climate Models. *Commun. Earth Environ.* **2025**, *6*, 75. [CrossRef]
57. Zhao, M.; Running, S.W. Drought-Induced Reduction in Global Terrestrial Net Primary Production from 2000 Through 2009. *Science* **2010**, *329*, 940–943. [CrossRef] [PubMed]
58. Reichstein, M.; Papale, D.; Valentini, R.; Aubinet, M.; Bernhofer, C.; Knohl, A.; Laurila, T.; Lindroth, A.; Moors, E.; Pilegaard, K.; et al. Determinants of Terrestrial Ecosystem Carbon Balance Inferred from European Eddy Covariance Flux Sites. *Geophys. Res. Lett.* **2007**, *34*, 1–21. [CrossRef]
59. Law, B.E.; Falge, E.; Gu, L.; Baldocchi, D.D.; Bakwin, P.; Berbigier, P.; Davis, K.; Dolman, A.J.; Falk, M.; Fuentes, J.D.; et al. Environmental Controls over Carbon Dioxide and Water Vapor Exchange of Terrestrial Vegetation. *Agric. For. Meteorol.* **2002**, *113*, 97–120. [CrossRef]
60. Jung, M.; Reichstein, M.; Margolis, H.A.; Cescatti, A.; Richardson, A.D.; Arain, M.A.; Arneth, A.; Bernhofer, C.; Bonal, D.; Chen, J.; et al. Global Patterns of Land-Atmosphere Fluxes of Carbon Dioxide, Latent Heat, and Sensible Heat Derived from Eddy Covariance, Satellite, and Meteorological Observations. *J. Geophys. Res. Biogeosciences* **2011**, *116*, G00J07. [CrossRef]
61. Robinson, C.; Dilkina, B.; Hubbs, J.; Zhang, W.; Guhathakurta, S.; Brown, M.A.; Pendyala, R.M. Machine learning approaches for estimating commercial building energy consumption. *Appl. Energy* **2017**, *208*, 889–904. [CrossRef]
62. Woldemariam, G.W.; Awoke, B.G.; Raian Vargas Maretto, R.V. Remote sensing vegetation Indices-Driven models for sugarcane evapotranspiration estimation in the semiarid Ethiopian Rift Valley. *ISPRS J. Photogramm. Remote Sens.* **2024**, *215*, 136–156. [CrossRef]
63. Raich, J.W.; Schlesinger, W.H. The Global Carbon Dioxide Flux in Soil Respiration and Its Relationship to Vegetation and Climate. *Tellus B* **1992**, *44*, 81–99. [CrossRef]
64. Balsamo, G.; Agusti-Panareda, A.; Albergel, C.; Arduini, G.; Beljaars, A.; Bidlot, J.; Blyth, E.; Bousserez, N.; Boussetta, S.; Brown, A.; et al. Satellite and In Situ Observations for Advancing Global Earth Surface Modelling: A Review. *Remote Sens.* **2018**, *10*, 2038. [CrossRef]
65. Wu, Z.; Ahlström, A.; Smith, B.; Ardö, J.; Eklundh, L.; Fensholt, R.; Lehsten, V. Climate Data Induced Uncertainty in Model-Based Estimations of Terrestrial Primary Productivity. *Environ. Res. Lett.* **2017**, *12*, 064013. [CrossRef]
66. Huang, C.; Sun, C.; Nguyen, M.; Wu, Q.; He, C.; Yang, H.; Tu, P.; Hong, S. Spatio-Temporal Dynamics of Terrestrial Net Ecosystem Productivity in the ASEAN from 2001 to 2020 Based on Remote Sensing and Improved CASA Model. *Ecol. Indic.* **2023**, *154*, 110920. [CrossRef]
67. Ji, S.; Ren, S.; Fang, L.; Chen, J.; Wang, G.; Wang, Q. Improved CASA-Based Net Ecosystem Productivity Estimation in China by Incorporating Developmental Factors into Autumn Phenology Model. *Remote Sens.* **2025**, *17*, 487. [CrossRef]
68. Wang, H.; Jia, G.; Zhang, A.; Miao, C. Assessment of Spatial Representativeness of Eddy Covariance Flux Data from Flux Tower to Regional Grid. *Remote Sens.* **2016**, *8*, 742. [CrossRef]
69. Järvi, L.; Rannik, Ü.; Kokkonen, T.V.; Kurppa, M.; Karppinen, A.; Kouznetsov, R.D.; Rantala, P.; Vesala, T.; Wood, C.R. Uncertainty of Eddy Covariance Flux Measurements over an Urban Area Based on Two Towers. *Atmos. Meas. Tech.* **2018**, *11*, 5421–5438. [CrossRef]
70. Wang, S.; Cui, D.; Wang, L.; Peng, J. Applying Deep-Learning Enhanced Fusion Methods for Improved NDVI Reconstruction and Long-Term Vegetation Cover Study: A Case of the Danjiang River Basin. *Ecol. Indic.* **2023**, *155*, 111088. [CrossRef]
71. Cheng, Q.; Xie, R.; Wu, J.; Ye, F. Deep Learning-Based Spatiotemporal Fusion Architecture of Landsat 8 and Sentinel-2 Data for 10 m Series Imagery. *Remote Sens.* **2024**, *16*, 1033. [CrossRef]
72. Liang, X.; Yu, S.; Meng, B.; Wang, X.; Yang, C.; Shi, C.; Ding, J. Multi-Source Remote Sensing and GIS for Forest Carbon Monitoring Toward Carbon Neutrality. *Forests* **2025**, *16*, 971. [CrossRef]

73. van Wees, D. *Global Fire Emissions Based on Native Resolution Satellite Data. Ph.D. Thesis, Research and Graduation Internal*; Earth Sciences Amsterdam Sustainability Institute: Amsterdam, The Netherlands, 2023.
74. Takeda, N.; Rowlings, D.; Parton, W.; Grace, L.; Day, K.; Nguyen, T.; Grace, P. Soil Carbon Sequestration Potential in Subtropical Grasslands Estimated by DayCent-CABBI. *Soil Sci. Soc. Am. J.* **2025**, *89*, e70003. [CrossRef]
75. Petropoulos, T.; Benos, L.; Busato, P.; Kyriakarakos, G.; Kateris, D.; Aidonis, D.; Bochtis, D. Soil Organic Carbon Assessment for Carbon Farming: A Review. *Agriculture* **2025**, *15*, 567. [CrossRef]

Disclaimer/Publisher's Note: The statements, opinions and data contained in all publications are solely those of the individual author(s) and contributor(s) and not of MDPI and/or the editor(s). MDPI and/or the editor(s) disclaim responsibility for any injury to people or property resulting from any ideas, methods, instructions or products referred to in the content.